Available online at www.sciencedirect.com
SCIENCE DIRECT
Polymer 46 (2005) 295–302
polymer
www.elsevier.com/locate/polymer

Influence of π-complexing agents on the anionic polymerization of styrene with lithium as counterion in cyclohexane. 3. Effect of tetraphenylethylene

Guoming Wang[a], Kristof Janssens[a], Chantal Van Oosterwijck[a], Alexander Yakimansky[b], Marcel Van Beylen[a,*]

[a]*Laboratory of Macromolecular and Physical Organic Chemistry, Catholic University of Leuven, Celestijnenlaan 200F, B-3001 Leuven, Belgium*
[b]*Laboratory of Thermostable Polymers, Institute of Macromolecular Compounds of the Russian Academy of Sciences, Bolshoi prospect 31, 199004 St Petersburg, Russian Federation*

Received 1 September 2004; received in revised form 9 November 2004; accepted 9 November 2004

Abstract

The propagation reaction in anionic polymerization of styrene with lithium as counterion in cyclohexane has been investigated for four different concentrations of tetraphenylethylene (TPhE) in the range of living end concentrations between 10^{-5} and 10^{-3} M at 20 °C. The values of the apparent dissociation constant of PStLi dimer and the weighted rate constants of all unassociated species were obtained for all four investigated concentrations of TPhE. The mechanism, already used in the case of durene, was also applied in this system and the values of the relevant absolute propagation rate constants of the two reactive monomeric species have been derived from the kinetic results. The absolute propagation rate constant of PStLi·TPhE is much lower than that of PStLi. The complexation constant of PStLi with one molecule of TPhE is more than 100 times larger than that of PStLi with one molecule of durene.

Keywords: Anionic polymerization; Kinetics and mechanism; Tetraphenylethylene

1. Introduction

The kinetics of anionic polymerization of styrene with lithium as a counter ion has been studied in a number of non-polar solvents, including benzene [1], toluene [2], cyclohexane [3]. In all these cases, a kinetic order of 0.5 with respect to the living end concentration of polystyryllithium (PStLi) has been found for the apparent polymerization rate constants. This behavior has been unambiguously attributed to the coexistence of dimeric associates, $(PStLi)_2$, with a small fraction of monomeric species, PStLi, only the latter being able to propagate [4–6]. The equilibrium between the dimeric and monomeric living chain ends is shifted towards monomeric species in the presence of different agents capable of complex formation with PStLi. Until now, four series of complexing agents have been investigated, including inorganic salt such as metal alkoxide [7,8] (μ-type), THF [9], dioxane [10], *N*,*N*,*N*′,*N*′-tetramethylethylene diamine (TMEDA) [11], tetramethyltetraazacyclotetradecan (TMTCT) [12] (σ-type), polyether metal alkoxides [13–15], lithium aminoalkoxides [16] (μ-σ type), 1,2,4,5-tetramethylbenzene (durene) [17], tetraphenylethylene (TPhE) (π-type).

In an earlier paper [17], the influence of durene, one of the π-type additives, on the anionic polymerization of styrene was studied. In this work, the effect of TPhE on the propagation rate of PStLi in cyclohexane at 20 °C was investigated in detail.

2. Experimental section

All the purifications were carried out under high vacuum.

* Corresponding author. Tel.: +32 163 27431; fax: +32 16 327990.
E-mail address: marcel.vanbeylen@chem.kuleuven.ac.be (M. Van Beylen).

0032-3861/$ - see front matter © 2005 Elsevier Ltd. All rights reserved.
doi:10.1016/j.polymer.2004.11.020

Styrene was dried by distillation from CaH_2 (2×) and distilled over oligomeric lithium polystyrene. Sec-BuLi was purified by a short-path vacuum distillation. Cyclohexane was refluxed with Na–K alloy, then stirred and degassed on the vacuum line, finally distilled over oligomeric lithium polystyrene. TPhE was firstly recrystallized from ethanol, then vacuum-sublimed and finally further dried on the high vacuum line.

Oligomeric lithium polystyrene used at the start of the reaction was obtained by the initiation of styrene with sec-BuLi in cyclohexane, and its measured molecular weight is 5000. The initial monomer concentration was such that for the lowest concentration of active centers the molecular weight after reaction was around 50,000 to 60,000. The kinetics of the propagation reaction was determined by following the disappearance of styrene spectrophotometrically at 291 nm on a Cary 2200 at 20 °C.

Quantum-chemical calculations of equilibrium structures and energies of TPhE complexes with the model living chain end, 1-phenyl-ethyllithium (HStLi), were performed using the DFT approach [18] implemented into the TURBOMOLE package [19] of ab initio quantum-chemical programs. BP86 set of potentials, consisting of Becke's exchange potential [20] and Perdew's correlation potential [21], was used with TURBOMOLE split valence plus polarization (SVP) basis sets [22] of 6-31G* quality. Detailed description of calculation methods is published in Part 2 of this series [23].

3. Results and discussion

Fig. 1 shows the effect of TPhE on the observed propagation rate of PStLi in cyclohexane at two nearly constant total living end concentrations, $C^* = 5.4 \times 10^{-4}$ M and $C^* = 2.5 \times 10^{-3}$ M.

At $C^* = 5.4 \times 10^{-4}$ M, the k_{obs}/C^* value decreases monotonically with increasing concentration of TPhE. At

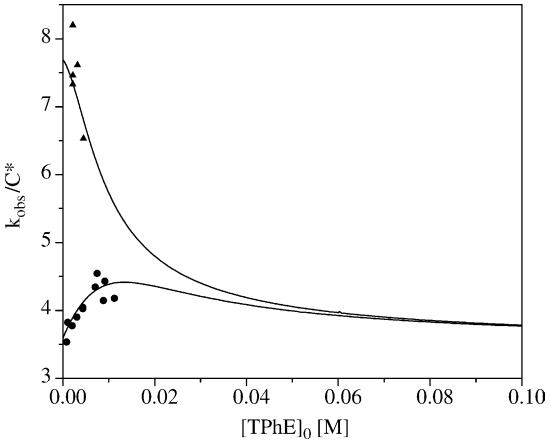

Fig. 1. The effect of TPhE on the propagation rate of PStLi in cyclohexane at 20 °C. (▲), $C^* = 0.54$ mM; (●), $C^* = 2.5$ mM; Solid line: calculated curve (the detailed procedures are shown in Appendix A).

$$(PStLi)_2 \underset{}{\overset{K_D}{\rightleftharpoons}} 2PStLi$$

$$PStLi + TPhE \overset{Ks_1}{\rightleftharpoons} PStLi \cdot TPhE$$

$$PStLi + Sty \xrightarrow{kp} (PSt)StyLi$$

$$PStLi \cdot TPhE + Sty \xrightarrow{kp_1} (PSt)StyLi \cdot TPhE$$

Scheme 1.

$$\text{Dimeric Species} \overset{K_D^{app}}{\rightleftharpoons} \text{Monomeric Species}$$

$$\text{Monomeric Species} + \text{Styrene} \xrightarrow{k_p^{app}} \text{Monomeric Species}$$

Scheme 2.

$C^* = 2.5 \times 10^{-3}$ M, it increases initially, passes through a maximum, and then decreases with increasing concentration of TPhE. A similar behavior has been found in the presence of durene (D) as the π-donor and it has been explained by the existence of three types of reactive species, PStLi, PStLi·D, and PStLi·2D [17]. However, extensive kinetic results and quantum chemical calculations seem to indicate that in the presence of TPhE, the observed non-monotonic dependence of k_{obs}/C^* on $[TPhE]_0$ is due to only two reactive monomeric species, as shown in Scheme 1.

In the presence of TPhE, the dissociative mechanism still holds, as shown in Scheme 2.

(K_D^{app} is the apparent dissociation constant of the PStLi dimers and k_p^{app} is the weighted rate constant of all non-associated species in the presence of TPhE analogous to the constants K_D and k_p in pure cyclohexane).

If only two monomeric species, PStLi and PStLi·TPhE, are involved into propagation reaction k_p^{app} can be defined as:

$$k_p^{app} = (1 - \alpha)k_p + \alpha k_{p_1} \tag{1}$$

where

$$\alpha = \frac{[PStLi \cdot TPhE]}{[PStLi] + [PStLi \cdot TPhE]} \tag{2}$$

Taking into account that

$$[PStLi \cdot TPhE] = K_{S_1}[PStLi][TPhE] \tag{3}$$

k_p^{app} is determined from Eqs. (1)–(3) by the following Eqs.:

$$k_p^{app} = \frac{k_p + K_{S_1}[TPhE]k_{p_1}}{1 + K_{S_1}[TPhE]} \tag{4}$$

On the other hand,

$$K_D^{app} = \frac{([PStLi] + [PStLi \cdot TPhE])^2}{[(PStLi)_2]} \tag{5}$$

Combining Eqs. (3) and (5), one can derive:

$$\sqrt{K_D^{app}} = \sqrt{K_D}(1 + K_{S_1}[TPhE]) \tag{6}$$

From Eqs. (4) and (6), it follows that:

$$\sqrt{K_D^{app}}k_p^{app} = \sqrt{K_D}(k_p + K_{S_1}[TPhE]k_{p_1}) \quad (7)$$

Combining material balance equation for TPhE

$$[TPhE] = [TPhE]_0 - [PStLi\cdot TPhE] \quad (8)$$

with

$$[PStLi\cdot TPhE] = K_{S1}[PStLi][TPhE] \quad (9)$$

one obtains:

$$[TPhE] = \frac{[TPhE]_0}{1 + K_{S1}[PStLi]} \quad (10)$$

As will be shown below, [PStLi] is very low at any value of $[TPhE]_0$. Thus, $K_{S1}[PStLi] \ll 1$ and $[TPhE] \approx [TPhE]_0$. Therefore, Eqs. (4), (6), and (7) may be rewritten as:

$$k_p^{app} = \frac{k_p + K_{S_1}[TPhE]_0 k_{p_1}}{1 + K_{S_1}[TPhE]_0} \quad (11)$$

$$\sqrt{K_D^{app}} = \sqrt{K_D}(1 + K_{S_1}[TPhE]_0) \quad (12)$$

$$\sqrt{K_D^{app}}k_p^{app} = \sqrt{K_D}(k_p + K_{S_1}[TPhE]_0 k_{p_1}) \quad (13)$$

According to Eq. (12), the values of K_D and K_{S1} can be determined from the plot of $\sqrt{K_D^{app}}$ vs. $[TPhE]_0$ by its intercept and slope, respectively. Similarly, Eq. (13) makes it possible to find the values of k_p and k_{p1} from the plot of $\sqrt{K_D^{app}}k_p^{app}$ vs. $[TPhE]_0$. Different $[TPhE]_0$, ranging from 1.2×10^{-3} M to 11.4×10^{-3} M were investigated and the detailed kinetic results are shown in Table 1.

For every particular $[TPhE]_0$ value, the values of k_p^{app} and K_D^{app} can be obtained from the intercept and slope, respectively, of the linear plot of C^*/k_{obs} vs. k_{obs} [24,25], as shown below:

$$\frac{C^*}{k_{obs}} = \frac{1}{k_p^{app}} + \frac{2k_{obs}}{(k_p^{app})^2 K_D^{app}} \quad (14)$$

The results are generalized in Table 2. At each constant $[TPhE]_0$, the experimental data fit the straight line very well, a typical example being shown in Fig. 2.

The data presented in Table 2 indicate that the K_D^{app} value increases and the k_p^{app} value decreases with increasing $[TPhE]_0$. In pure cyclohexane, the K_D value has been estimated to be of the order of 10^{-7} to 10^{-6} M [17]. The addition of TPhE increases the K_D^{app} value several orders, e.g. to 0.15 mM at $[TPhE]_0 = 1.2$ mM and 1.69 mM at $[TPhE]_0 = 4.5$ mM. These results prove that TPhE strongly enhances the dissociation of the PStLi dimers into the monomeric species.

Using the calculated K_D^{app} and k_p^{app} values, one can reconstruct the experimental dependence of $\log k_{obs}$ vs. $\log C^*$. For all $[TPhE]_0$ values, the calculated dependences of $\log k_{obs}$ vs. $\log C^*$ are in a very good agreement with the experimental data, as shown in Fig. 3 for $[TPhE]_0 =$ 3.2 mM.

A slight downward curvature of the bilogarithmic plot of k_{obs} vs. C^* in Fig. 3 shows a decrease of the reaction order from 0.72 at $C^* = 7.0\times10^{-5}$ M to 0.64 at $C^* = 3.3\times10^{-3}$ M. This is due to the coexistence of non-propagating PStLi dimers and propagating monomeric species in the presence of TPhE. The mole fraction of monomeric species decreases with increasing C^*, according to the following equation:

$$\frac{[monomeric]}{C^*} = \frac{-K_D^{app} + \sqrt{(K_D^{app})^2 + 8C^*K_D^{app}}}{4C^*} \quad (15)$$

The dependences of the mole fractions of the monomeric species on C^* for four different concentrations of TPhE are given in Fig. 4. It is clearly seen that the mole fraction of monomeric species increases with increasing amounts of TPhE at a constant C^* value.

Knowing the values of K_D^{app} and k_p^{app} determined at four

Table 1
Kinetic results of styrene polymerization in cyclohexane with lithium as a counter ion in the presence of tetraphenylethylene at 20 °C

$[TPhE]_0$ (mM)	C^* (mM)	k_{obs} (10^{-3} min^{-1})	k_{obs}/C^* (M^{-1} min^{-1})
1.2	0.05	0.95	19.00
	0.089	1.5	16.85
	0.25	2.6	10.40
	0.30	3.1	10.33
	0.73	4.5	6.16
	0.94	5.0	5.32
	2.8	10.4	3.71
	3.7	12.2	3.30
2.2	0.086	1.0	11.63
	0.09	0.9	10.00
	0.45	3.3	7.33
	0.50	4.1	8.20
	0.67	5.0	7.46
	0.80	4.4	5.50
	0.97	6.0	6.19
	1.0	6.0	6.00
	1.5	7.3	4.87
	2.9	10.0	3.45
	3.0	11.3	3.77
3.2	0.098	1.2	12.24
	0.075	0.8	10.67
	0.12	1.1	9.17
	0.46	3.5	7.61
	1.26	6.8	5.40
	2.15	9.9	4.60
	3.3	12.2	3.89
4.5	0.21	1.8	8.57
	0.58	3.8	6.53
	1.54	7.2	4.68
	2.0	6.86	3.43
	3.0	12.0	4.00
7.2	3.0	13.0	4.64
7.6	2.2	9.07	4.12
9.0	2.2	7.44	3.38
9.3	2.0	9.28	4.64
10.0	2.5	8.46	3.38
11.4	2.4	10.0	4.17

Table 2
Summary of the values of K_D^{app} and k_p^{app}

$[TPhE]_0$ (mM)	K_D^{app} (mM)	k_p^{app} (M^{-1} min^{-1})
1.2	0.15	24.69
2.2	0.39	16.05
3.2	0.82	12.74
4.5	1.69	9.61

different concentrations of TPhE, one is able to find the dependences of $\sqrt{K_D^{app}}$ vs. $[TPhE]_0$ and $\sqrt{K_D^{app}}k_p^{app}$ vs. $[TPhE]_0$, as shown in Figs. 5 and 6.

Fitting the plots in Figs. 5 and 6 according to the linear Eqs. (12) and (13), respectively, results in the values of $K_D = 2.4\times10^{-7}$ M, $K_{S1} = 18{,}000\,M^{-1}$, $k_p = 520\,M^{-1}\,min^{-1}$, $k_{p1} = 3.5\,M^{-1}\,min^{-1}$. With these values, it is possible to calculate the dependence of k_p^{app} vs. $[TPhE]_0$ (Eq. (11)) and to compare it with the experimental data. Such a comparison presented in Fig. 7 clearly shows an excellent agreement between calculated and experimental results.

Moreover, the validity of the determined values of these parameters can be checked by fitting the original experimental data of k_{obs}/C^* vs. $[TPhE]_0$ (the detailed calculation procedures are shown in the Appendix A). The calculation result is shown in Fig. 1 (solid line) at $C^* = 5.4\times10^{-4}$ M and 2.5×10^{-3} M. The simulated lines reproduce the original dependences very well. It can also be seen from Fig. 1 that at sufficiently high concentrations of TPhE, unreachable in actual practice, a common line will result for the two C^* values, indicating that all the dimeric species are dissociated and complexed. This region of concentrations of TPhE, where the polymerization reaction is of first order in C^*, starts from $[TPhE]_0 = 0.05$ M. This concentration is beyond the maximum solubility of TPhE in cyclohexane (around 0.01 M). Therefore, the reaction order will never be

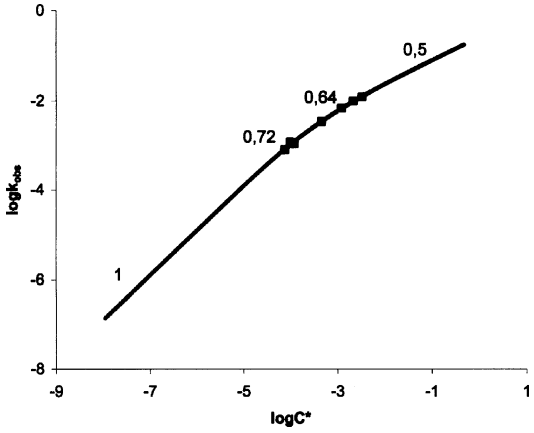

Fig. 3. Dependence of log k_{obs} vs. log C^* at $[TPhE]_0 = 3.2$ mM. ((■), experimental points, solid line is calculated with $K_D^{app} = 0.824$ mM, $k_p^{app} = 12.74\,M^{-1}\,min^{-1}$).

entirely unity within all the investigated concentrations of TPhE.

It is important to note that the determined values of K_D, K_{S1}, k_p, k_{p1} make it possible to calculate the concentrations of the three ionic species, $(PStLi)_2$, PStLi, and PStLi·TPhE, involved in the presence of TPhE, as shown in Fig. 8.

With increasing $[TPhE]_0$, the concentration of dimeric chain end aggregates, $(PStLi)_2$, decreases gradually, approaching zero at $[TPhE]_0 > 0.04$ M, and the concentration of monomeric complexed chain ends, PStLi·TPhE, increases monotonically, leveling off in the same region of $[TPhE]_0$. The concentration of monomeric non-complexed chain ends, PStLi, is always very low and becomes practically zero at $[TPhE]_0 > 0.02$ M.

To further test the complexing dissociating capacity of π-donors, we tried to synthesize the *cis*-dimethylstilbene, but were unable to obtain it free from the *trans*-isomer. On the other hand, we also investigated the propagation of

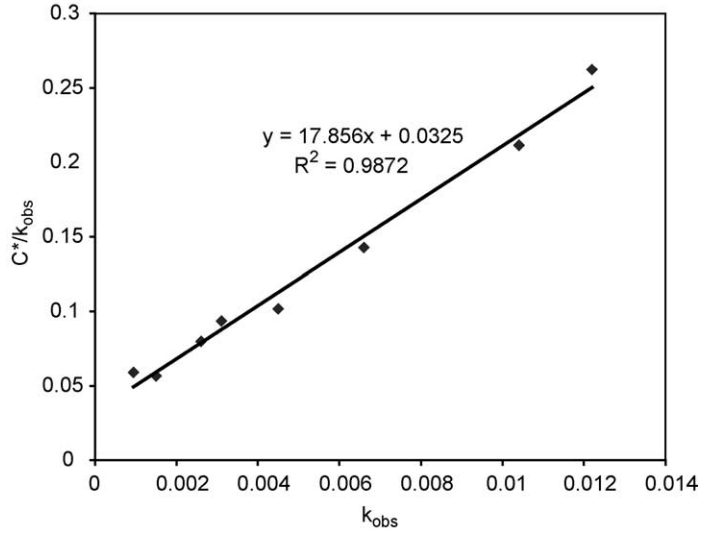

Fig. 2. Plot of C^*/k_{obs} vs. k_{obs} at $[TPhE]_0 = 3.2$ mM.

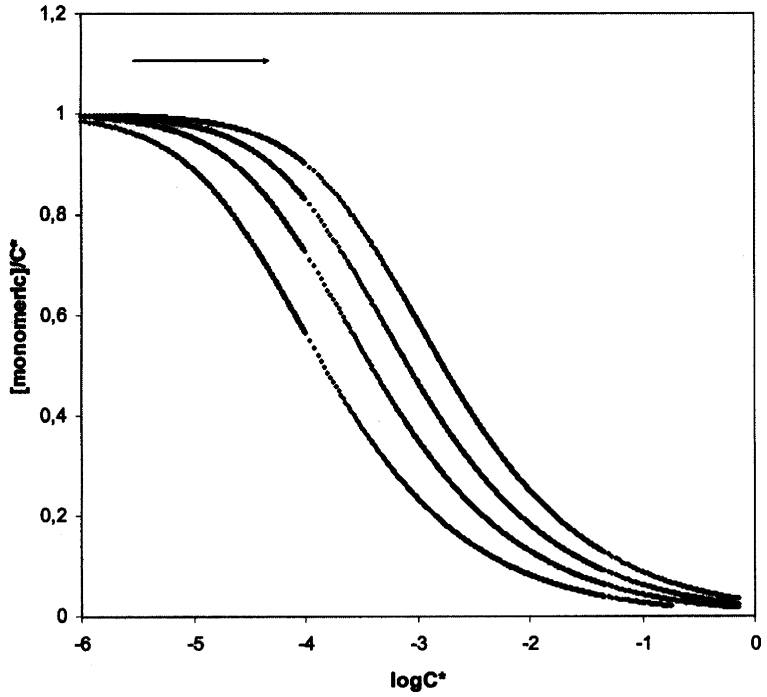

Fig. 4. Dependences of the mole fraction of the monomeric species on C^* at four different concentrations of TPhE. $[TPhE]_0 = 1.2$, 2.2, 3.2, 4.5 mM, respectively, in the direction of the arrow.

PStLi in the presence of 1,3,5-tri-*t*-butylbenzene and found that it is not metallated by organolithium compounds, as is durene in the long run. However, 1,3,5-tri-*t*-butylbenzene gives only somewhat higher values of k_{obs}/C^* and a slightly earlier maximum in the k_{obs}/C^* vs. [π-donor] plot than observed in the presence of durene [17]. Thus, the ability of 1,3,5-tri-*t*-butylbenzene to induce the dissociation of $(PStLi)_2$ dimers is nothing comparable with that of TPhE. We therefore did not pursue the investigation any further.

It should be noted that the equilibrium constant value $K_{S1} = 18{,}000\ M^{-1}$ calculated above for the complex formation between PStLi and TPhE is more than two orders of magnitude higher than that found in the presence of durene as the π-complexing agent ($140\ M^{-1}$, [17]). Thus, the difference, $\Delta\Delta G$, between the reaction free energies, ΔG, for the interactions of PStLi with durene and TPhE should be about 2.7 kcal/mol. Of course, there should be entropic contributions, $\Delta\Delta S$, to the estimated $\Delta\Delta G$ value because TPhE, in contrast to durene, is able to form several types of complexes with PStLi. Indeed, we found four different types of HStLi·TPhE complexes (Fig. 9) with the

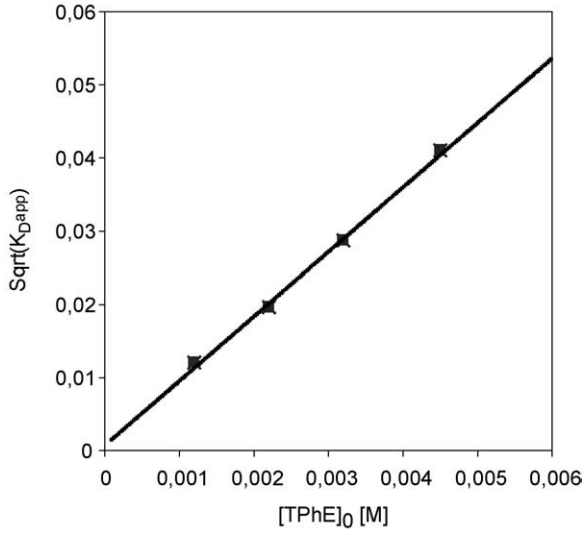

Fig. 5. Plot of $\sqrt{K_D^{app}}$ vs. $[TPhE]_0$ ((■), experimental points, solid line-simulated results, according to Eq. (12)).

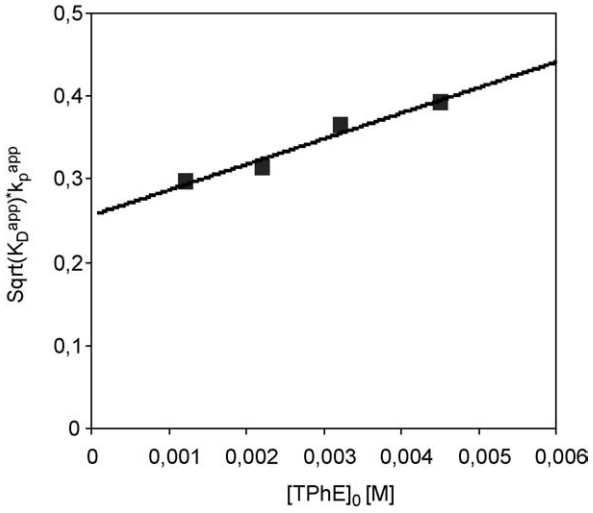

Fig. 6. Plot of $\sqrt{K_D^{app} k_p^{app}}$ vs. $[TPhE]_0$ ((■), experimental points, solid line-simulated results, according to Eq. (13)).

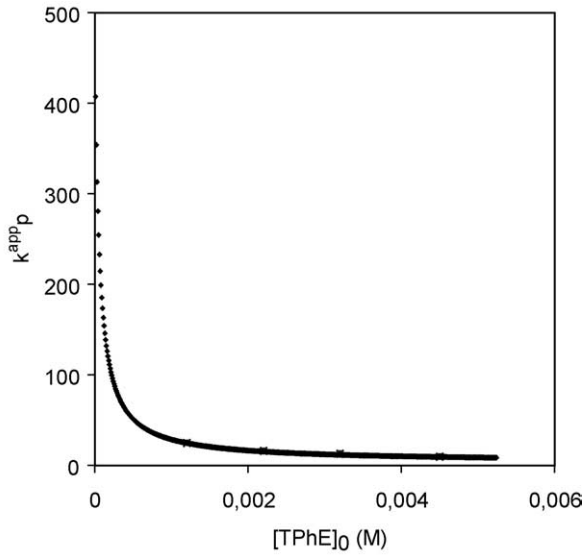

Fig. 7. Plot of k_p^{app} vs. $[TPhE]_0$ ((■), experimental points, solid line-simulated results, according to Eq. (11) with the determined values of $k_p = 520\ M^{-1}\ min^{-1}$, $k_{p1} = 3.5\ M^{-1}\ min^{-1}$, and $K_{S1} = 18{,}000\ M^{-1}$).

calculated total energies (at the BP86/SVP level of theory) within the range of 0.0025 Hartree = 1.5 kcal/mol. One can see that the Li–C bond of the model chain end, HStLi, is either approximately perpendicular (Fig. 9(a) and (d)) or nearly parallel (Fig. 9(b) and (c)) to the C=C bond of TPhE. Moreover, if perpendicular to the C=C bond of TPhE, the Li-C bond of HStLi, can be either almost parallel (Fig. 9(a)) or perpendicular (Fig. 9(d)) to the plane of the ethylene fragment of TPhE. In these four complexes, one of phenyl rings of TPhE is closer to the Li–C bond of HStLi than the others. This selected phenyl ring can be any of the four phenyl rings of TPhE. Thus, the number of different configurations of complexes between TPhE and PStLi is 16. However, only one type of the HStLi·D complex has been found in which the Li–C bond of the model chain end is nearly perpendicular to the aromatic ring plane of durene molecule (Fig. 2(a) in Ref. [23]). Thus, the number of different configurations of complexes between durene and PStLi is 2, because PStLi can be arranged below and above the plane of a durene molecule. It is possible to estimate that $T\Delta\Delta S = RT \cdot \ln(16/2) = 1.2$ kcal/mol at 20 °C. It means that there should be ca. 1.5 kcal/mol of enthalpic contribution to the $\Delta\Delta G$ value. However, according to our previous quantum-chemical DFT calculations, the chain end complex with TPhE is not more stable than that with durene [23]. Probably, the relative stabilities of the PStLi complexes with TPhE are underestimated with respect to the complexes between PStLi and durene by at least 1.5 kcal/mol, which is well within the range of rms error for the employed DFT method (about 4 kcal/mol [26]).

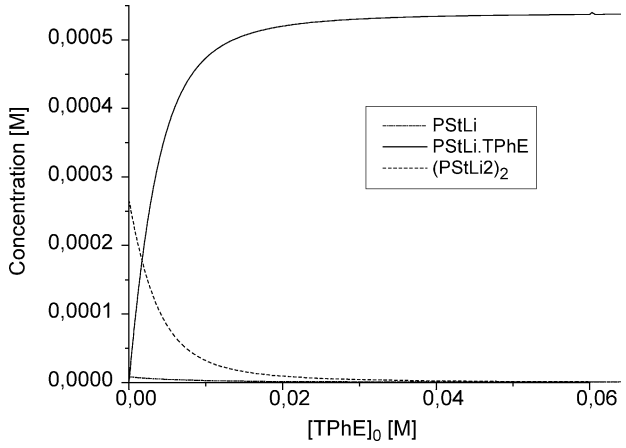

Fig. 8. Calculated concentration of ionic species in the presence of TPhE ($C^* = 0.54$ mM).

4. Conclusions

The influence of TPhE on the anionic polymerization of styrene with lithium as a counterion in cyclohexane was investigated. At low total concentration of living ends ($C^* = 5.4 \times 10^{-4}$ M), the observed propagation rate constant decreases monotonically with increasing concentration of TPhE. At high concentration of living ends ($C^* = 2.5 \times 10^{-3}$ M), the increase of $[TPhE]_0$ gives rise to an increase in the observed propagation rate constant, which passes through a maximum and then decreases with the further addition of TPhE. This is explained by the coexistence of non-propagating dimeric chain ends and two reactive monomeric species, i.e. non-complexed and complexed with one TPhE molecule.

Within the investigated region of $[TPhE]_0$, the plot of log k_{obs} vs. log C^* is curved, indicating a change in the order with respect to the total living ends concentration. The reaction order with respect to the active centers is found in all cases to be greater than 0.5, which is attributed to the dissociation of the dimers, $(PStLi)_2$, into the monomeric species, PStLi and PStLi·TPhE. The mole fraction of monomeric species is quantitatively calculated and increases with increasing amount of TPhE. In comparison with the situation in pure cyclohexane, the apparent dissociation constant, K_D^{app}, increases while the weighted rate constant, k_p^{app}, decreases with the increase in $[TPhE]_0$. Based upon the extensive kinetic study, the values of the absolute propagation rate constants of each monomeric species involved are derived. The absolute propagation rate constant of PStLi·TPhE, k_{p1}, is much lower than that of PStLi, k_p. The complexation constant, K_{S1}, of PStLi with one TPhE molecule is more than 100 times larger than that of PStLi with one molecule of durene.

5. Supplementary material

Z-matrices and HYPERCHEM.hin files of the optimized structures of the complexes HStLi·TPhE.

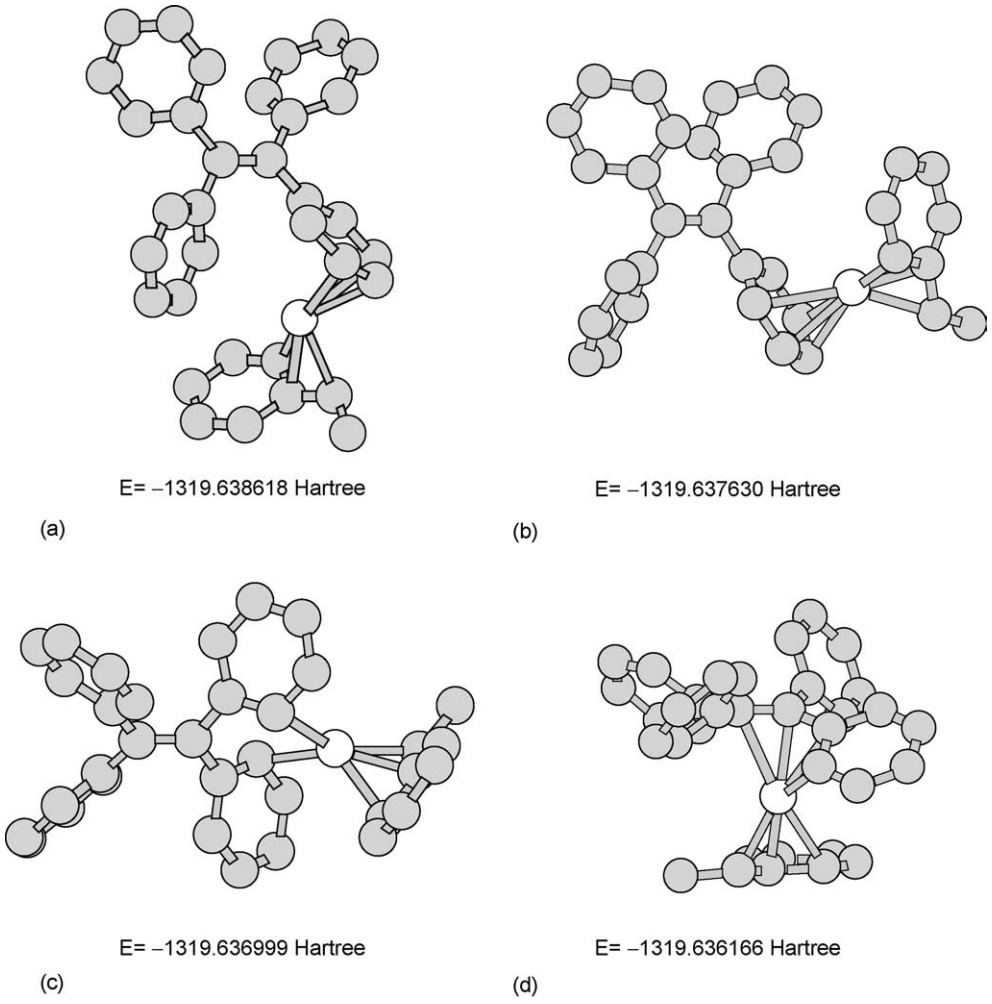

Fig. 9. Optimized geometries of the StLi complexes with TPhE molecule. Carbon atoms are gray, lithium atoms are white, hydrogen atoms are not shown. C–Li contacts shorter than 2.65 Å are shown as valence bonds. Total energies, *E*, calculated at the BP86/SVP level of theory are presented.

Acknowledgements

We wish to express our gratitude to Katholieke Universiteit Leuven for the financial support and for a fellowship for two of us (G.W. and K.J.).

Appendix A

Assuming [PStLi] = B, it follows from $K_D = \frac{([PStLi])^2}{[(PStLi)_2]}$ that

$$[(PStLi)_2] = \frac{B^2}{K_D} \tag{A1}$$

From Eqs. (8) and (10):

$$[PStLi \cdot TPhE] = \frac{K_{S1}[TPhE]_0 B}{1 + K_{S1}B} \tag{A2}$$

On the other hand,

$$2[(PStLi)_2] + [PStLi] + [PStLi \cdot TPhE] = C^* \tag{A3}$$

Combining Eqs. (A1), (A2), and (A3), one arrives at:

$$\frac{2B^2}{K_D} + B + \frac{K_{S1}[TPhE]_0 B}{1 + K_{S1}B} = C^*$$

Then the final expression is:

$$2K_{S1}B^3 + (2 + K_D K_{S1})B^2 + (K_D + K_D K_{S1}[TPhE]_0 - K_D K_{S1} C^*)B - K_D C^* = 0 \tag{A4}$$

Taking $K_D = 2.4 \times 10^{-7}$ M and $K_{S1} = 18{,}000\ M^{-1}$, for two constant total concentrations of living ends, that is, $C^* = 2.5 \times 10^{-3}$ M and 5.4×10^{-4} M, the value of B can be accordingly calculated by Mathematica software. The value of [PStLi·TPhE] can also be obtained by Eq. (A2). Finally, taking $k_p = 520\ M^{-1}\ min^{-1}$ and $k_{pI} = 3.5\ M^{-1}\ min^{-1}$, the observed propagation rate constant can be found from the expression:

$$k_{obs} = k_p[PStLi] + k_{p1}[PStLi \cdot TPhE]$$

Appendix B. Supplementary data

Supplementary data associated with this article can be found, in the online version, at doi:10.1016/j.polymer.2004.11.020.

References

[1] Worsfold DJ, Bywater S. Can J Chem 1960;38:1891.
[2] Spirin YuL, Gantmakher AR, Medvedev SS. Dokl Akad Nauk SSSR 1962;46:368.
[3] Johnson AF, Worsfold DJ. J Polym Sci, Part A 1965;3:449.
[4] Szwarc M, Van Beylen M. Ionic polymerization and living polymers. London: Chapman and Hall; 1993.
[5] Van Beylen M, Bywater S, Smets G, Szwarc M, Worsfold DJ. Adv Polym Sci 1988;86:87.
[6] Hsieh HL, Quirk RP. Anionic polymerizaiton, principles and pratical applications. New York: Marcel Dekker; 1996.
[7] Roovers JEL, Bywater S. Trans Faraday Soc 1966;62:1876.
[8] Hsieh HL. J Polym Sci, Part A 1 1970;8:533.
[9] Bywater S, Worsfold DJ. Can J Chem 1962;40:1564.
[10] Bywater S, Alexander IJ. J Polym Sci 1968;6:3107.
[11] Fontanille M, Helary G, Szwarc M. Macromolecules 1988;21:1532.
[12] Helary G, Fontanille M. Polym Bull 1980;3:159.
[13] Bayard P, Jérôme R, Teyssié Ph, Varshney S, Wang JS. Polym Bull 1994;32:381.
[14] Wang JS, Jérôme R, Teyssié Ph. J Phys Org Chem 1995;8:208.
[15] Zune C, Jérôme R. Prog Polym Sci 1999;24:631.
[16] Hon Chiu Leung. Master's thesis, Catholic University Leuven; 1999.
[17] Wang G, Van Beylen M. Polymer 2003;44:6205.
[18] Parr RG, Yang W. In: Density-functional theory of atoms and molecules, 333. Oxford, England: Oxford University Press; 1989. p. 333.
[19] Ahlrichs R, Bär M, Häser M, Horn H, Kölmel C. Chem Phys Lett 1989;162:165.
[20] Becke AD. Phys Rev A 1988;38:3098.
[21] Perdew JP. Phys Rev B 1986;33:8822.
[22] Schäfer A, Horn H, Ahlrichs R. J Chem Phys 1992;97:2571.
[23] Yakimansky A, Wang G, Janssens K, Van Beylen M. Polymer 2003;44:6457.
[24] Bywater S. Prog Polym Sci 1994;19:287.
[25] Duda A, Penczek S. Macromolecules 1994;27:4867.
[26] Frisch MJ, Trucks GW, Cheeseman JR. Recent developments and applications of modern density functional theory. In: Seminario JM, editor. Theoretical and computational chemistry 4. Amsterdam: Elsevier; 1996. p. 679–707.